ORGANIC CHEMISTRY FRONTIERS

RESEARCH ARTICLE

View Article Online
View Journal | View Issue

Cite this: *Org. Chem. Front.*, 2022, **9**, 649

Catalytic properties of 4,5-bridged proline methano- and ethanologues in the Hajos–Parrish intramolecular aldol reaction†

Sofiane Hocine, ‡[a] Gilles Berger, ‡[b] K. N. Houk [c] and Stephen Hanessian *[a]

Received 9th November 2021,
Accepted 30th November 2021

DOI: 10.1039/d1qo01688a

rsc.li/frontiers-organic

The catalysis of the Hajos–Parrish reaction by *cis*- and *trans*-4,5-ethano-proline was explored experimentally and computationally with DFT (ωB97X-D and MN15) and DLPNO-CCSD(T). Both of the new catalysts are as active as proline or *cis*- and *trans*-4,5-methano-proline, with the *trans*-ethano-proline being as enantioselective as proline. A thorough theoretical analysis of the electronic factors influencing catalysis is reported.

Introduction

In the early 70's, two historically relevant papers, published independently by scientists at Hoffmann-La Roche[1,2] and Schering AG[3] marked the beginning of what we currently know as organocatalysis.[4,5] Hajos and Parrish described the highly stereoselective intramolecular aldol reaction of a prochiral triketone **1** using L-proline as a catalyst. The quasi enantiopure product **2** bearing an α-ketol functionality was dehydrated to the (*S*)-perhydroindanedione **3** that is a valuable chiral synthon (chiron) for the synthesis of a variety of complex natural products harboring an angular methyl group on a stereogenic carbon atom (Scheme 1).[6,7] This early landmark achievement was preceded by studies by Yamada[8,9] who reported the first example of the use of L-proline esters as a catalyst in the asymmetric Michael additions of cyclohexanone enamines to methyl acrylate achieving optical yields as high as 59%. Since then, a large body of work has been done to exploit the remarkable ability of L-proline to engage in catalytic asymmetric reactions to create enantiomerically enriched, if not pure, carbogenic compounds.[10] The 2021 Nobel Prize in chemistry was awarded in part for the pioneering contributions of Benjamin List using proline as an organocatalyst. Inspired by the development of antibodies for catalytic aldol reactions, List, Lerner, and Barbas, found proline to be remarkably effective for a simple intermolecular aldol reaction.[11] The mechanism of the proline-catalyzed aldol reaction has been a topic of great experimental and computational interest over the years.[11–15] Insights into transition states of enamine-based aldol reactions with proline were reported by Bahmanyar and Houk in 2001[14] and List in 2004.[15] In a seminal paper, List and Houk elucidated the source of stereoselectivity in the intermolecular reaction.[16] This work demonstrated the importance of combining theoretical methods with experimental results.[17] A DFT study of the direct aldol reaction between acetone and acetaldehyde by Boyd highlighted the role of the solvent in stabilizing charged intermediates.[18] Further refinements of the mechanism by DFT calculations have been recently reported by Tafida and coworkers.[19]

Clemente and Houk delineated the mechanism of the proline-catalyzed Hajos–Parrish asymmetric reaction leading to the perhydroindenedione **3**.[20] According to the Houk-List "one-proline model",[16] the enamine resulting from the condensation with the exocyclic carbonyl group in the triketone **1** can adopt either *anti* or *syn* orientations to the carboxylic acid group (Fig. 1). The proton transfer from the acid promotes enamine attack on the ketone,[20] and the stereochemistry is determined by the preference for the enamine to be *anti* to the

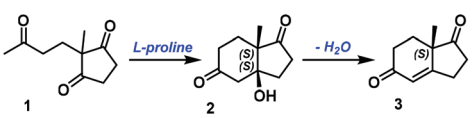

Scheme 1 The L-proline catalyzed Hajos–Parrish–Eder–Sauer–Wiechert reaction, leading to the chiral perhydroindanedione **3**.

[a]*Department of Chemistry, Université de Montréal, Station Centre-Ville, C.P. 6128, Montreal, QC, H3C 3J7, Canada. E-mail: stephen.hanessian@umontreal.ca*
[b]*Microbiology, Bioorganic & Macromolecular Chemistry, Faculty of Pharmacy, Université Libre de Bruxelles, Bd du Triomphe, 1050 Brussels, Belgium*
[c]*Department of Chemistry and Biochemistry, University of California, Los Angeles, CA 90095-1569, USA*

†Electronic supplementary information (ESI) available. CCDC 2100195–2100197 and 2100194. For ESI and crystallographic data in CIF or other electronic format see DOI: 10.1039/d1qo01688a

‡These authors contributed equally.

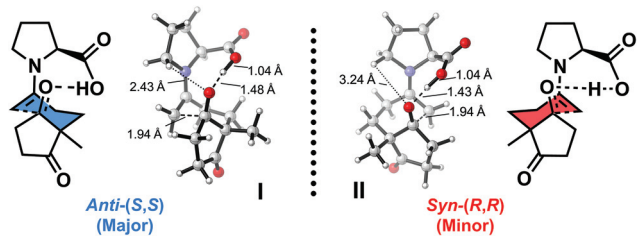

Fig. 1 The *anti* (I) and *syn* (II) transition states leading to both cyclized enantiomers **2**-(*S*,*S*) and **2**-(*R*,*R*).

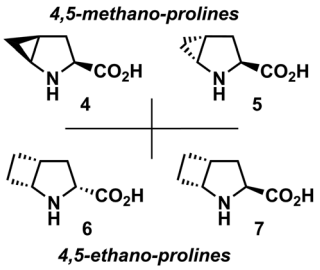

Fig. 2 The *cis*- and *trans*-4,5-methano-prolines (**4**,**5**) and the homologous *cis*-and *trans*-ethano-prolines (**6**,**7**).

acid. This would facilitate the geometry of proton transfer from the carboxylic acid, to afford a more planar forming iminium, and to bring the developing alkoxide near the partially positive CH α to the developing iminium.[16,21] The possible stabilizing role of the $NC^5H^{\delta+}\cdots O^{\delta-}$ interaction with the carbonyl oxygen in the transition structures was initially invoked in the case of proline.[20] A priori, this was a plausible hypothesis in view of the shorter calculated distance of 2.4 Å in the case of the *anti*-transition structure (**I**) compared to over 3 Å for the *syn* structure (**II**) (Fig. 1).

In previous studies we reported that 4,5-methano-L-prolines were catalytically competent in the Hajos–Parrish reaction.[22] The higher enantioselectivity (93% ee) provided by *cis*-4,5-methano-L-proline **4** compared to the *trans*-isomer **5** (82% ee) was rationalized based on the conformational preferences of the respective proline derivatives to achieve a transition structure that would favor a planar enamine geometry (*vide infra*). It was anticipated that the NC^5 methine-H in the *trans*-congener **5** would be favorably oriented to interact with the developing alkoxide, which in combination with hydrogen bond donation from the carboxylic acid group, would lead to the highly enantioenriched cyclization product **3** after dehydration. As in the case of proline, the calculated distance of 2.5 Å in the *SS-anti*-transition structure was favorable compared to the *syn*-enamine transition structure (3.5 Å).[22,23] Hanessian had initially observed flattening of the pyrrolidine ring of the *cis*-congener **4** in the crystalline solid state possibly resulting from potential steric repulsion of the carboxylic acid group with the cyclopropane ring.[24] This led Cheong and Houk to suggest a more planar enamine geometry that allows an easier transition to the *anti*-iminium transition structure (Fig. 6B).[22,23] They further inferred that the *trans*-4,5-methano-L-proline **5** would be more likely to adopt a boat-like conformation that would negatively affect the planarity of the enamine. The observed stereoinduction of 84% ee would arise mainly from the interaction of the carboxyl group with the developing alkoxide with minimal involvement of the NC^5 methine hydrogen atom.

In view of the importance of the geometry of the transition structures and their dependence on conformational factors associated with the constrained 4,5-methano-prolines, we were interested to investigate the catalytic properties of a higher homologue represented by the *cis*- and *trans*-4,5-ethano-L-prolines **6** and **7** in the Hajos–Parrish reaction (Fig. 2). Since the conformations of the pyrrolidine rings would be more flexible compared to the methano congeners, we also wanted to further probe the possible role that the NC^5 methine hydrogens and other proximal *endo*-hydrogens might play in stabilizing the transition structures in the respective *cis*- and *trans*-4,5-ethano-L-proline congeners. We studied the stereoselectivity of the reaction comparing the two pairs of 4,5-methano- and 4,5-ethano-L-prolines as catalysts by modern DFT, coupled-cluster calculations and energy decomposition analysis. With the added information provided by the 4,5-ethano-L-prolines and the energy decomposition of the various transition structures, we propose a refined model highlighting the importance of steric repulsion in the *syn*-(*R*,*R*) transition structures for the overall enantioselectivity of the reaction. We also took the opportunity to revisit the transition structures involved in the now venerable L-proline-catalyzed Hajos–Parrish reaction.

Results and discussion

Synthesis of the 4,5-bridged proline analogues

cis- and *trans*-4,5-methano-L-proline (**4**,**5**) were obtained as previously reported.[25–28] *cis*-4,5-Ethano-D-proline and *trans*-4,5-ethano-L-proline (**6**,**7**) were prepared by adopting standard methods (see ESI†) and obtained as crystalline solids (Fig. 3). The extensive flattening of the pyrrolidine ring in the proline methanologues[29] **4** and **5** highlighted by an increased sp^2-character of the C_5–N and C_5–H bonds,[30] is no longer present in the ethano derivatives, probably due to the added flexibility provided by the ethano-bridge.[24,30]

We were surprised to see a strong 1 ppm downfield shift on the C^5 proton resonance, as well as more than a 10 ppm shift for the ^{13}C resonance, in comparison to methano-proline (Fig. 3). These observations are however in agreement with a theoretical study by Stojanovic.[31] The unshielded H^5 may help to stabilize the *trans*-4,5-ethano-L-proline *anti*-TS, in which it interacts with the forming alkoxide. On the contrary, methano-prolines displayed more shielded C^5 resonances (around 35 ppm). The pyrrolidine ring adopts an *endo* pucker with C^1 outside of the plane in the two ethano-proline diastereomers, in contrast to proline for which puckering is seen for C^3 and for which *endo* and *exo* puckers are both populated as observed in crystal structures of amino acids and peptides.[32,33]

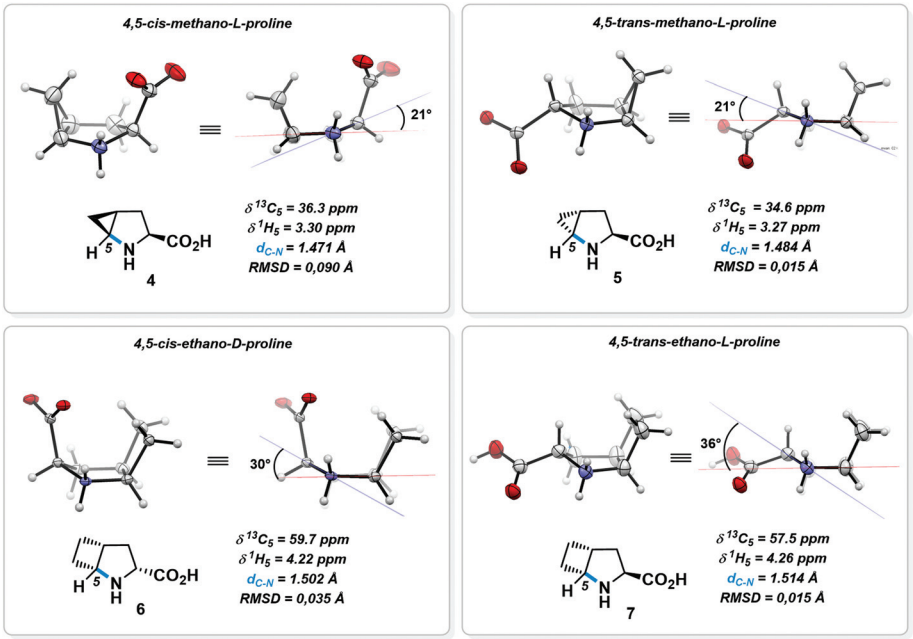

Fig. 3 X-ray structures of *cis*- and *trans*-4,5-(m)ethano prolines **4**, **5**, **6** and **7**. Selected distances and NMR chemical shifts.

Catalytic efficiency

The conversion of triketone **1** to the hydroxy perhydroindanedione **2** was monitored by ^{1}H-NMR spectroscopy (Fig. 4). Both the *cis*- and *trans*-4,5-ethano-prolines **6** and **7** were competent catalysts in conversion of the triketone **1** to the cyclized product **2**. The *trans*-4,5-L-ethano catalyst **7** performed equally well compared to proline itself (98% *vs.* 97% ee) in contrast to the *cis*-D-ethano diastereomer **6** (64% ee) (Table 1). In spite of the difference in stereoselective induction, both catalysts exhibited the same conversion time as proline. Interestingly, the higher asymmetric induction previously observed with *cis*-4,5-methano-L-proline **4** compared to the *trans* isomer **5**[22] was now reversed for the ethano-bridged proline catalysts.

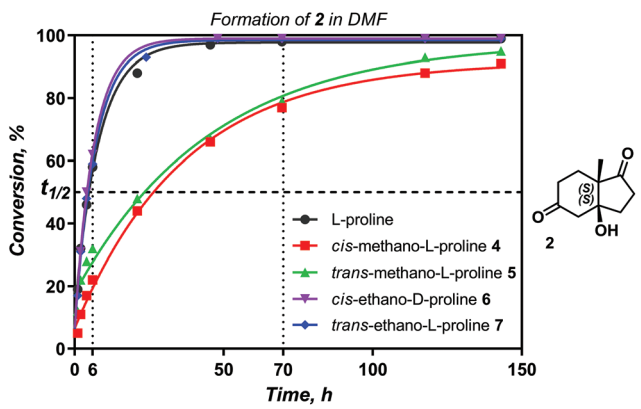

Fig. 4 Hajos–Parrish reaction time course for L-proline and the 4,5-bridged methano- and ethanologues, as monitored by evolution of ^{1}H-NMR signals corresponding to the cyclized product **2**.

Table 1 Yields and %ee values for the Hajos–Parrish reaction, catalyzed by L-proline and the 4,5-bridged analogues

	Conversion (%)			
Catalyst	6 h	70 h	$t_{1/2}$ (h)	ee (%)
L-Proline	58	98	5.5	97
cis-Methano-L-proline **4**	22	77	25.6	93
trans-Methano-L-proline **5**	32	79	31.7	83
cis-Ethano-D-proline **6**[a]	62	99	4.5	64[b]
trans-Ethano-L-proline **7**	59	99	4.8	98

[a] See ESI.† [b] The opposite enantiomer is formed.

The proline and 4,5-methano-L-proline catalyzed reactions were experimentally and computationally studied more than a decade ago by Houk and Hanessian.[20,22] Similar to proline, the *anti*-(*S*,*S*) TS structure has been shown to be favored *versus* the *syn*-(*R*,*R*) structure, no matter the stereochemistry of the fused cyclopropane ring (Fig. 6). Very recently, 7-azabicyloalkane carboxylic acid amides were reported as organocatalysts in intermolecular aldol reactions by Wojaczyńska and coworkers[34] (dr 22 : 78, ee up to 63%). Based on *in silico* DFT studies, Sinisha and Sunoj predicted enantiomeric excesses in the range 85–92% in the aldol reaction between acetone and *p*-nitrobenzaldehyde catalyzed by conformationally rigid azabicyclic amino acids.[35]

Analysis of the transition states

Computational models and resources have evolved since the first studies by Houk.[14,20] For proline, the free energy difference between the two diastereomeric transition structures

($\Delta G^{\ddagger}_{TS\text{-}syn} - \Delta G^{\ddagger}_{TS\text{-}anti}$) had been calculated by Houk and co-workers to be around 2 kcal mol^{-1},[21–23] using the B3LYP exchange–correlation functional with Pople basis sets.[22] Using the ωB97x-D and MN15 functionals, the $\Delta\Delta G^{\ddagger}$ are calculated at 3.0 and 2.0 kcal mol^{-1}, respectively using the dispersion-corrected ωB97x-D and the global hybrid MN15 exchange–correlation functionals,[36] with the polarized triple-zeta basis set def2-TZVP, and a continuum solvation model for DMF.[37,38] This is in agreement with Houk's early results.[21–23] Bonding analysis reveals a late transition state that better resembles an iminium alkoxide rather than the starting enamine. An hyperbond, as implemented in the NBO program,[39] is found between the two carbons forming the new bond and the oxygen from the ketone acceptor. The electron density of this hyperbond is partitioned for two thirds between the two carbons closing the cycle and a third on the C–O axis (Fig. 5).

We then repeated the previous calculations for the *cis*- and *trans*-4,5-methano-L-prolines **4** and **5**. Our results consistently showed a favorable *anti*-(*S*,*S*) transition state, similar to the previously reported energies.[22] The dispersion-corrected calculations for the methano-prolines (ωB97x-D) also predict a better asymmetric induction for the *cis*-methano analogue (Fig. 6A). Dihedrals around the enamine in the diastereomeric transition states consistently reveal a more planar enamine for the *anti*-(*S*,*S*) transition structures (*i.e.* low χ_N, **4a** and **5a**, Fig. 6B). For both methano catalysts, the *anti*-enamine TS also allows for better NC^{5}H$^{\delta+}\cdots$O$^{\delta-}$ interactions, as highlighted by the shorter NC^{5}H–O distances. In the case of the *cis*-4,5-methano-L-proline, an added NC^{5}H contact with the carboxylic acid oxygen exists. Thus, making two contacts, one with the alkoxide and one with the carboxyl. To further investigate these NC^{5}H–O contacts, we looked at the amount of charge transfer (CT) to the σ* antibonding C^5–H using NBO perturbative estimates of donor–acceptor interactions (NBO_{CT}). We can note that, in the 4,5-*cis*-methano *anti*-TS **4a**, a 0.6 kcal mol^{-1} CT stabilization through NC^{5}H$\cdots$O delocalization is calculated with the carboxylic oxygen, but none with the developing alkoxide. The *cis*-methano *syn*-TS **4b** does not profit much from such interaction, which is quantified at 0.2 kcal mol^{-1}. For the *trans*-4,5-methano-L-proline, neither of the **5a** or **5b** TS display this CT stabilization with the carboxyl, although a small (0.2 kcal mol^{-1}) NC^{5}H$\cdots$O delocalization is seen with the alkoxide in the *anti*-enamine TS **5a**. These observations corroborate the C^{5}H$\cdots$O distances and highlight added stabilization of the *anti*-enamine TS in the case of the *cis*-4,5-methano-L-proline.

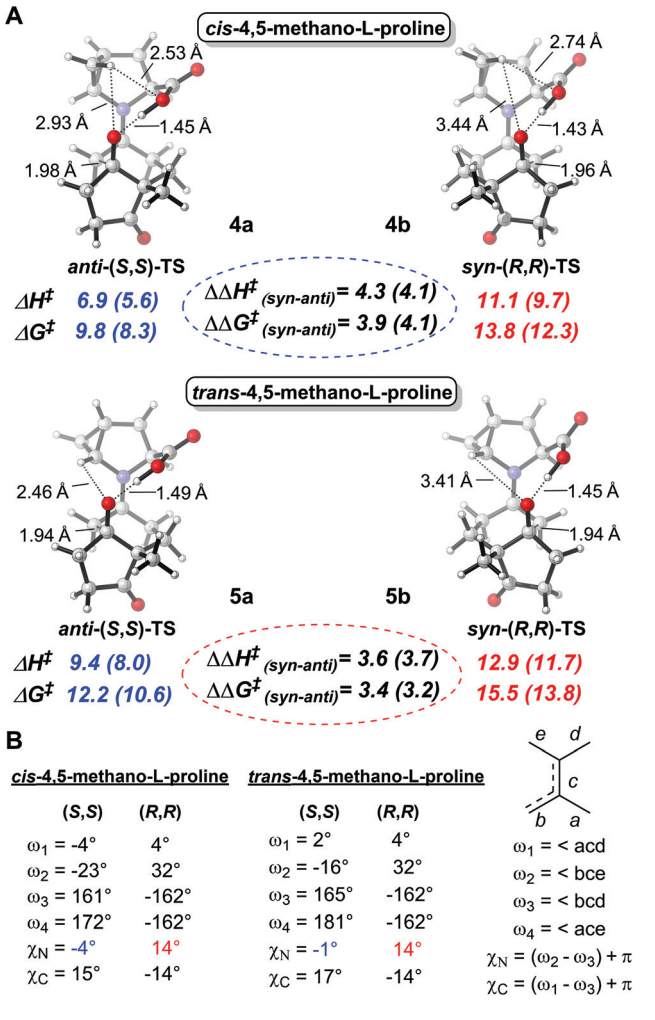

Fig. 6 A: Activation energies for the diastereomeric transition states obtained from the *cis*- and *trans*-4,5-methano-L-proline at the ωB97x-D/def2-TZVP level of theory, energies in DMF (MN15 energies are given between brackets). B: Dihedrals around the C–N bond and pyramidalization of the iminium.

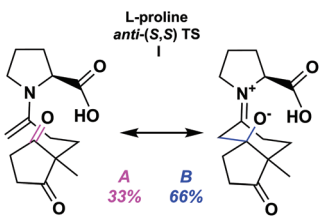

Fig. 5 Proportions of the two resonances structures in the L-proline *anti*-(*S*,*S*)-TS **I**, as described by the hyperbond search within the NBO program.

Similar calculations, run with the ωB97x-D and MN15 functionals, were conducted for the 4,5-ethano-proline analogues to predict and verify their catalytic performance in the Hajos–Parrish reaction in comparison to the previously calculated parameters for 4,5-methano derivatives[22] and in light of the new experimental results (Fig. 7A). The *trans*-4,5-ethano-L-proline **7** was found to produce a more disfavored *syn*-(*R*,*R*)-enamine TS when compared to its *cis*-diastereomer **6**, which is in agreement with the observed ee (98 *vs.* 64% ee). This is highlighted by the $\Delta\Delta G^{\ddagger}$s (2.5 *vs.* 3.4 kcal mol^{-1} for the *cis*- and *trans*-ethano-prolines, **6** and **7** respectively) and is further evident in the gas phase, where the $\Delta\Delta G^{\ddagger}$s are even better split ($\Delta\Delta G^{\ddagger}$ = 2.3 *vs.* 4.6 kcal mol^{-1} for the *cis*- and *trans*-4,5-ethano-prolines **6** and **7**, respectively).

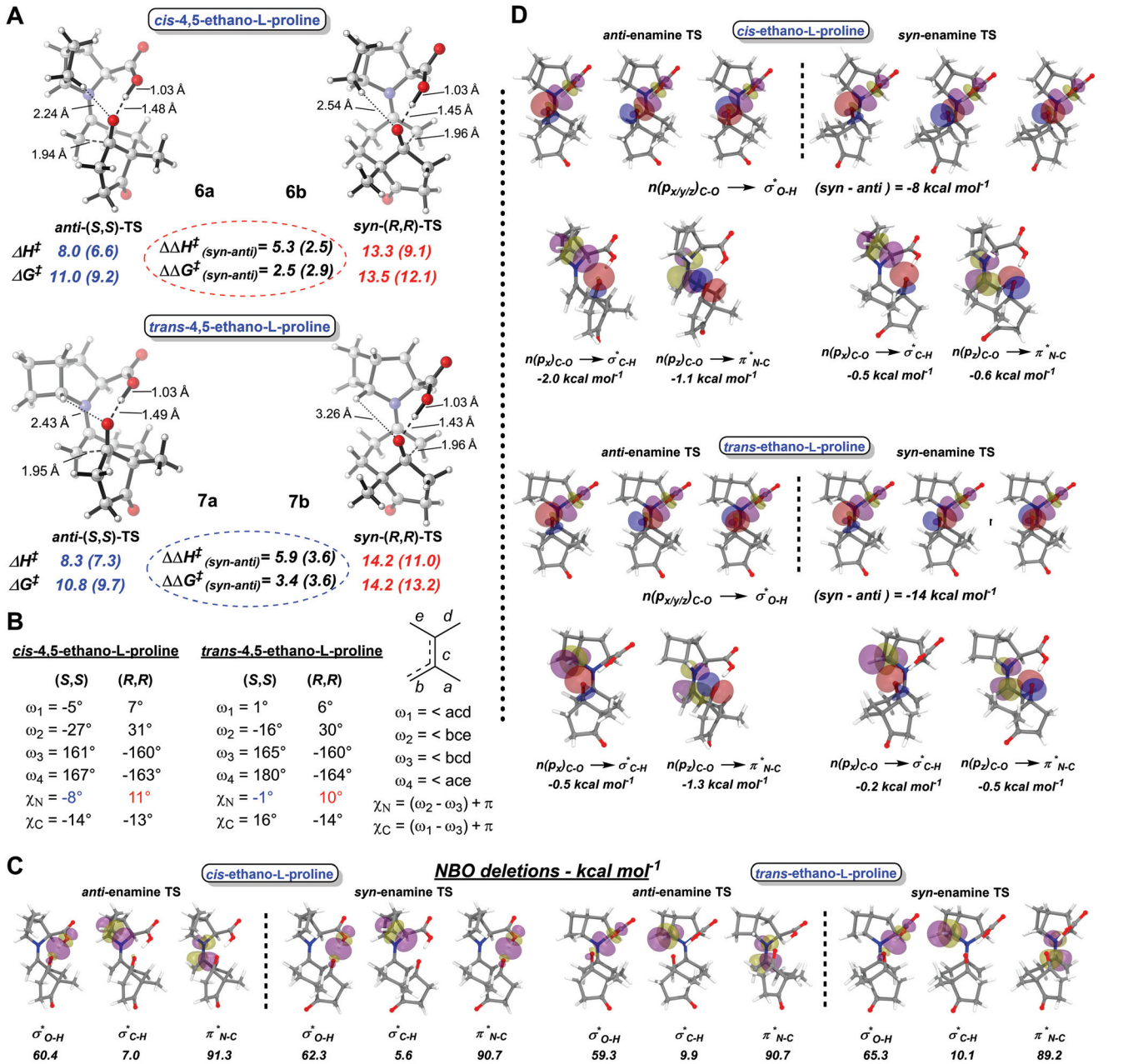

Fig. 7 A: Activation energies for the diastereomeric transition states for the *cis*- and *trans*-4,5-ethano-L-proline catalysts (ωB97x-D/def2-TZVP, energies in DMF). MN15 energies are given between brackets. B: Dihedrals around the enamine/iminium transition state, showing the favorable planar conformation (χ_N = –1°) for the *trans*-4,5-ethano-L-proline **7**. C: NBO deletions of relevant acceptor orbitals. D: NBO donor–acceptor delocalizations (NBO_{CT}) around the reaction center for the *syn*- and *anti*-transition states for both *cis*- and *trans*-4,5-ethano-L-proline catalysts.

For the *trans*-4,5-ethano-L-proline **7**, which is the best catalyst of the series, the O···H distance between the C^5–H and the carbonyl oxygen is significantly shorter in the *anti*-(*S*,*S*)-enamine TS **7a** than in the *syn*-(*R*,*R*)-enamine TS **7b** (2.43 Å *vs.* 3.26 Å, Fig. 7A), providing better stabilization to the developing alkoxide, in line with the proline and methano-proline catalysts. This is further evidenced by the NBO evaluation of the charge transfer (NBO_{CT} 0.5 *vs.* 0.2 kcal mol^{-1} for the *anti*-(*S*,*S*)-enamine TS *vs.* the *syn*-(*R*,*R*)-enamine TS, Fig. 7D). However, deleting the σ* C–H acceptor orbital does not produce significant differences between the *anti* and *syn*-enamine TS (increase in energy is 9.9 *vs.* 10.1 kcal mol^{-1} for the *anti* and *syn*-TS, respectively, Fig. 7C), considering that this orbital is also accepting electron density from nearby donors other than the C–O lone pairs. The quasi-ideal −1° pyramidalization in the *anti*-TS, reflects on the planarity of the enamine. In an attempt to evaluate the effect of the planarity of the enamine/iminium on the electron accepting properties of the antibonding π* C–N and the resulting stabilization to the TS, we calculated the NBO_{CT} between the alkoxide lone pairs and the anti-

bonding π* C–N, showing increased NBO_{CT} stabilization for the *anti*-enamine TS (1.3 *vs.* 0.5 kcal mol^{-1}, Fig. 7D). Deletion of this acceptor orbital shows that it further stabilizes the *anti*-TS by 1.5 kcal mol^{-1} in comparison to the *syn*-TS (Fig. 7C). These increased $NC^5H\cdots O$ (lp → σ*) and O···C=N (lp → π*) CT stabilizations in the *anti*-TS are also seen for proline (see ESI†). Finally, the extent of charge transfer (CT) from the alkoxide to the carboxyl O–H σ* is stronger in the *syn*-enamine TS, hence the shorter distance of 1.43 Å *vs.* 1.49 Å (Fig. 7A).

For the *cis*-4,5-ethano-L-proline, the *anti*-TS is no longer favored by a more planar enamine (χ_N = −8° and 11° for **6a** and **6b**) which correlates with the poor asymmetric induction (64% ee). C^5–H interactions with the alkoxide are still present but now with the methylene hydrogen of the ethano bridge. The $C^5H\cdots O$ distances are rather similar (2.24 Å *vs.* 2.54 Å for the *anti*-(*S*,*S*)-enamine TS **6a** and the *syn*-(*R*,*R*)-enamine TS **6b**, Fig. 7A), which contrasts with the methano-proline and *trans*-ethano-proline cases (Fig. 6A). Charge transfer estimates between the alkoxide lone pair and the C^5–H σ* highlight a stronger $NC^5H\cdots O$ stabilization for the *anti*-enamine TS, in line with the 2.4 and 3.3 Å distances (NBO_{CT} 2.0 *vs.* 0.5 kcal mol^{-1} for the *anti*-(*S*,*S*)-enamine TS *vs.* the *syn*-(*R*,*R*)-enamine TS, Fig. 7D). Deletion of this σ* C–H acceptor orbital gives a little higher increase in energy for the *anti*-(*S*,*S*)-enamine TS (7.0 *vs.* 5.6 kcal mol^{-1} for the *anti* and *syn*-TS, respectively, Fig. 7C), whereas deletion of the σ* O–H from the carboxyl shows higher O···H–O NBO_{CT} stabilization in the *syn*-TS (in agreement with the shorter distance and similar to the *trans*-ethano case). Similar energy changes arise from the deletion of the π* N–C acceptor orbital in the *syn*-(*R*,*R*) and *anti*-(*S*,*S*)-enamine TS, in accordance with the comparable dihedrals found around the C–N bound for the two *cis*-4,5-ethano-L-proline TS. NBO charge transfer and specific deletions therefore helped us to confirm and quantify the importance of the interactions between the forming alkoxide, the carboxyl and, depending on the catalyst, the C5 or methylene hydrogen.

To further quantify the refinement of the TS energies, we turned to Domain-based Local Pair Natural Orbital (DLPNO)-CCSD(T) calculations. The DLPNO approach renders feasible the nearly complete coupled-cluster calculations including single, double and approximated triple excitations on large molecules. This permits comparisons of rather accurate wave-function calculations to the DFT calculations described so far.[40–42] The DLPNO-CCSD(T) electronic energies were used with DFT geometries and thermochemical corrections, and these results are listed in the ESI.† DLPNO-CCSD(T) consistently predicts a marked preference for the *trans*-4,5-ethano-L-proline isomer **7** *versus* the *cis*-isomer **6** in terms of asymmetric induction ($\Delta\Delta G^{\ddagger}$ 3 kcal mol^{-1}), but surprisingly fails at predicting the methano-proline case. The *trans*-4,5-methano-L-proline **5** has a slightly higher $\Delta\Delta G^{\ddagger}$, although the difference between the *cis*- and *trans*-4,5-methano-L-proline catalysts **4** and **5** is very small (around 0.5 kcal mol^{-1}). This is reflected in the DFT and the experimental ee, since the catalysts **4** and **5** do not produce such a strong split of the diastereomeric TS as seen with the 4,5-ethano-L-prolines **6** and **7**. A closer look at the energies reveals that the discrepancy may arise from an overestimation of the activation barrier to the *syn*-enamine TS for the *trans*-4,5-methano-L-proline (19.4 and 19.2 kcal mol^{-1}, depending on the starting geometries), which resulted in a higher predicted ee. Thus, in our case, the DLPNO-CCSD(T) approach did not predict the experimental ee, probably due to the use of DFT geometries and thermochemical corrections with single point DLPNO-CCSD(T) electronic energies.

Energy decomposition

Another method to discriminate between relative energies of TSs is with energy decomposition analysis. To gain further insight in the divergent asymmetric inductions between the *cis* and *trans*-ethano-prolines, we analyzed the *syn*- and *anti*-enamine TS for all catalysts using energy decomposition as provided in the NBO program.[43–45] The energies of the transition structures were decomposed into the main energetic contributions arising from electrostatics, steric interactions and quantum orbital interaction effects (eqn (1)). These are, in other terms, the classic-like electrical component of the Coulomb interactions (E_{EL}), the steric exchange arising from Pauli repulsions between filled orbitals energy (E_{SX}) and the charge transfer component due to the acceptor–donor "delocalization" interactions between filled and empty orbitals, as seen in Fig. 7 (E_{CT}).

$$E = E_{Coulomb} + E_{steric} + E_{quantum} \quad (1)$$

$$E = E_{EL} + E_{SX} + E_{CT} \quad (2)$$

These energy components are extremely large compared to the subtle differences in total energies and must be viewed with some caution. We first looked at proline as a reference in the Hajos–Parrish reaction for further comparison with methano- and ethano-prolines. The results in Table 2 indicate that the preferred *anti*-enamine TS is less susceptible to steric effects, whereas the *syn*-enamine TS-isomer experiences stronger Pauli repulsion between filled orbitals. Therefore, in the *syn*-enamine TS, the stronger overall CT energy only partially balances the electrostatic and steric handicap, resulting in an overall 4.5 kcal mol^{-1} difference in the electronic energy. As discussed earlier for the ethano-proline derivatives, the strongest CT interactions arise from the overlap of the alkoxide lone pairs to the σ* orbital of the carboxylic acid and these are stronger for the *syn*-enamine TS.

We then proceeded with the analysis of the methano- and ethano-proline catalysts. The energy decomposition shows that the *trans*-ethano-proline *syn*-enamine TS **7b** is handicapped by

Table 2 Energy decomposition analysis and comparison between the *syn* and *anti* TS using L-proline as catalyst in the Hajos–Parrish reaction. The *anti*-TS is taken as reference and therefore set as zero

	E_{EL}	E_{SX}	E_{CT}	E
L-Proline *anti*-enamine TS **I**	0	0	0	0
L-Proline *syn*-enamine TS **II**	5.5	19.9	−20.9	4.5

Table 3 Energy decomposition analysis and comparisons between the *syn*- and *anti*-enamine TS for the 4,5-bridged proline analogues. The *anti*-TS are taken as reference and therefore set as zero

		E_{EL}	E_{SX}	E_{CT}	E
cis-Methano	*anti*-TS **4a**	0	0	0	0
	syn-TS **4b**	0.4	39.3	−36.0	3.7
trans-Methano	*anti*-TS **5a**	0	0	0	0
	syn-TS **5b**	−1.7	11.8	−6.5	3.6
cis-Ethano	*anti*-TS **6a**	0	0	0	0
	syn-TS **6b**	0.4	−21.9	24.5	3.0
trans-Ethano	*anti*-TS **7a**	0	0	0	0
	syn-TS **7b**	−0.6	38.1	−33.0	4.5

large steric repulsion (38.1 kcal mol^{-1} more than the *anti*-enamine TS **7a**), while the *cis*-ethano-proline has a sterically favored *syn*-enamine TS but lower CT stabilization than the *anti*-enamine TS (Table 3). A similar pattern is also found for the methano-prolines, for which both *syn*-enamine TS are penalized by steric effects only partly compensated by electronic delocalizations and coulombic interactions. These steric effects disfavoring the *syn*-enamine TS are less pronounced in the case of the *trans*-methano-L-proline, which correlates with this analogue to be a poorer chiral inducer compared to the *cis*-isomer.

These energy decomposition analyses highlight an inverse tendency between the methano and ethano catalysts, which correlates with the experimental reversal of efficiency between the diastereomeric series.

Formation of reactive enamines and "parasitic" oxazolidinones

The existence of a reactive enamine intermediate that precedes the C–C bond formation is clearly established, but the pathway to enamines from reactants and the possible involvement of other species are still somewhat debated.[46–50] Early on during their mechanistic studies of using proline in aldol reactions, Seebach and Eschenmoser gave a detailed account of the catalytic cycle recognizing that iminium intermediates could be in equilibrium with oxazolidinones.[49] Blackmond and coworkers have also invoked oxazolidinones as precatalysts in proline-catalyzed reactions.[50] The interplay between different transition states in conjunction with the formation of iminiums, enamines and oxazolidinones from proline and a ketone is shown as a model in Scheme 2.[49,51] The efficiency of the proline catalyzed aldol reactions could be affected by such species hence the term 'parasitic' intermediates.

To complete our analysis, we looked at the steps preceding the final ring closure event, namely the formation of enamines and oxazolidinones. Two major pathways have been proposed: direct formation of enamines from the iminium or through intramolecular cyclization to oxazolidinone intermediates.[46,48,49]

We also considered the involvement of oxazolidinones as intermediates in the catalytic cycle of the Hajos–Parrish reaction using 4,5-methano and 4,5-ethano-prolines as catalysts. First, the enthalpies and free energies along the reaction pathways to the *syn*- and *anti*-enamines for all catalysts were calculated and are given in Table 4.

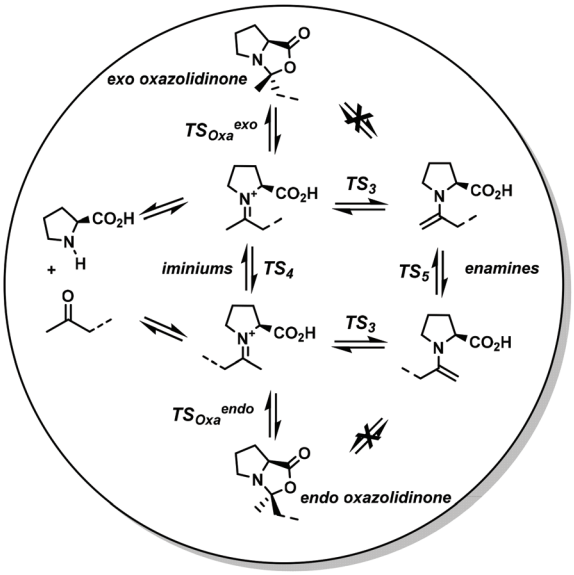

Scheme 2 Interconversion between iminiums, oxazolidinones and enamines.

The enthalpies, free energies and structures of the intermediates and transition states of the reaction enroute to the enamines through carbinolamines and iminiums for both ethano-proline catalysts are reported in Fig. 8.

The free energies to TS_1 are similar for the formation of both carbinolamines (*i.e.*, *syn* and *anti* pathway), and this within the entire series of catalysts, with a slight preference for the *syn* carbinolamine in the case of proline and *cis*-methano-proline, while that is reversed in the *trans*-methano case (Fig. 8A/B and Table 4). The computed structures of all TS, together with their O–H, C–O and C–N distances (breaking and forming bonds) are given in Fig. 8C and D. The second step (TS_2), which involves the loss of water and formation of the iminium intermediate, is always faster for the *anti* pathway, no matter the catalyst or its stereochemistry (Fig. 8A/B). This discrepancy is reduced for the *trans*-ethano-proline **7** in comparison to its *cis* isomer ($\Delta\Delta G^{\ddagger}_{TS_2(syn-anti)}$ = 3.3 *vs.* 5.5 kcal mol^{-1}, from the carbinolamines (Fig. 8A/B and Table 4). The last step toward the enamines (TS_3) consists in a proton transfer from the methyl iminium to the carboxylate, either by directly in the case of the *syn*-pathway (*i.e.* from the *E* iminiums) or through proton shuttling by a water molecule in the case of the *anti* pathway (*i.e.* from the *Z* iminiums), as seen in Fig. 8C and D. For this last step to enamine formation, the geometry around the C=N center becomes critical, especially for the distance between methyl protons and the carboxylate oxygen. This results in divergent activation energies to TS_3, which in the case of the *Z*-iminiums requires the intervention of a water molecule to transfer the proton between the remote groups (as seen for both TS_3^{anti} in Fig. 8C/D). This makes the TS_3 always higher for the *anti* pathway by around 6 to 10 kcal mol^{-1} for all catalysts (Table 4). The energy barriers from the

Table 4 DFT energies for the formation of the enamine intermediates with proline and the 4,5-methano- and ethano-L-proline catalysts, for both pathways leading to the *syn* and *anti* enamines (ωB97x-D/def2-TZVP)

G (H)		TS_1	Carbinolamine	TS_2	iminium	TS_3	enamine
L-Proline	*syn*	17.6 (11.6)	10.2 (4.7)	19.6 (13.6)	0.6 (7.4)	16.9 (21.6)	5.9 (11.7)
	anti	19.3 (14.3)	11.2 (6.6)	15.4 (10.9)	0.2 (8.7)	23.0 (19.3)	7.5 (14.8)
cis-Methano **4**	*syn*	17.7 (13.0)	9.8 (5.9)	18.7 (13.8)	−0.8 (8.1)	15.8 (23.0)	7.7 (15.7)
	anti	21.7 (16.4)	13.5 (8.2)	17.5 (12.2)	2.5 (10.2)	25.6 (20.8)	10.1 (17.2)
trans-Methano **5**	*syn*	21.3 (17.1)	10.8 (6.5)	22.2 (18.0)	2.7 (11.5)	14.3 (22.6)	7.0 (15.0)
	anti	19.3 (15.5)	10.4 (6.3)	16.0 (11.5)	0.9 (9.5)	24.6 (20.7)	7.5 (15.5)
cis-Ethano **6**	*syn*	20.1 (12.6)	11.7 (4.6)	20.3 (12.5)	2.4 (7.9)	18.9 (23.4)	8.3 (14.5)
	anti	20.0 (15.7)	10.8 (6.9)	14.8 (11.1)	0.1 (9.9)	23.1 (20.3)	7.2 (16.0)
trans-Ethano **7**	*syn*	16.6 (11.1)	9.2 (4.5)	17.5 (12.8)	−2.2 (6.1)	14.7 (21.5)	3.6 (12.0)
	anti	17.5 (13.4)	9.0 (5.0)	14.2 (10.1)	−1.0 (8.3)	22.3 (18.9)	6.7 (14.7)

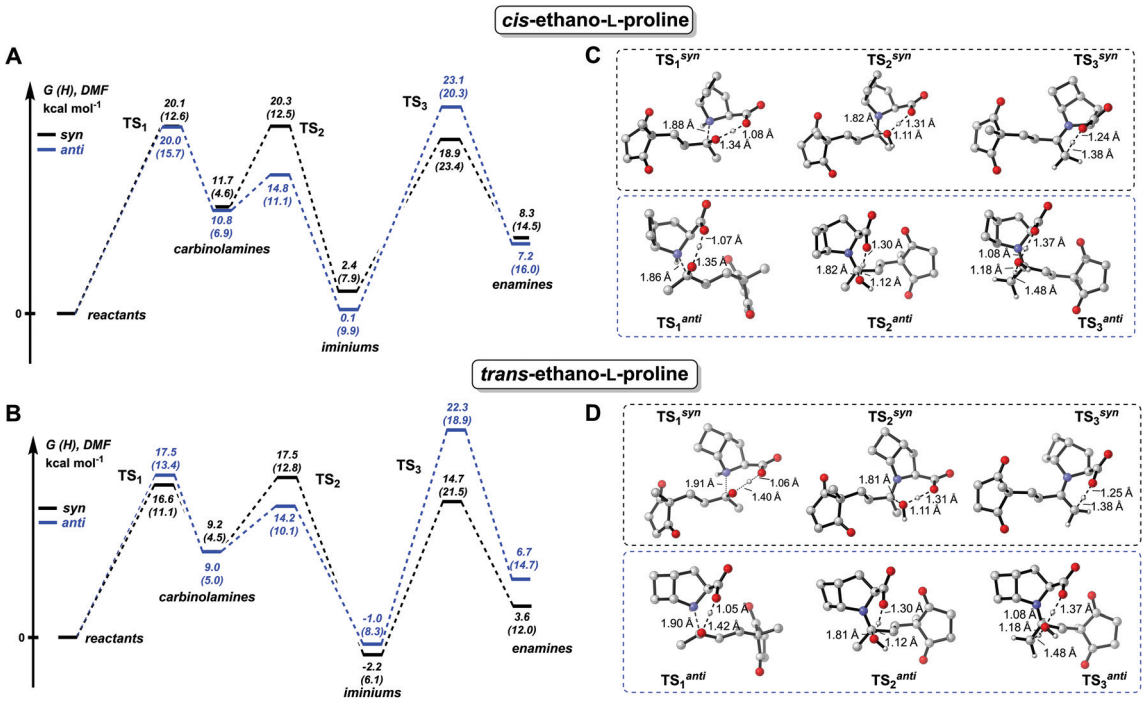

Fig. 8 A and B: DFT energy profile for the formation of the *syn*- and *anti*-enamines using *cis*- (A) and *trans*-ethano-proline (B) as catalysts (ωB97x-D/def2-TZVP, in DMF). B and D: Structures of the transition states for the *syn*- and *anti*-pathways for the *cis*- and *trans*-4,5,ethano-prolines. It is worth noting that the *anti*-enamine pathway involves a water-assisted proton transfer for the last step.

Z-iminiums to the *anti* enamines are all found around 23–25 kcal mol^{-1} and these limit the formation of the *anti*-enamines at room temperature (Fig. 8A/B and Table 4). The more accessible *syn*-enamines would then isomerize to the *anti*-conformation.

Our observations are in line with recent high level calculations from Gschwind *et al.* on the proline-catalyzed self-aldolization of 3-methylbutanal.[51]

Experimental detection and evidence have demonstrated the formation of oxazolidinones from the iminium intermediates,[47] but direct involvement of these bicyclic species in the key steps of the proline-catalyzed aldol reaction is not backed up by theoretical evidence. Direct generation of enamines from the oxazolidinones would involve higher energy steps than from iminiums.[51] For the Seebach mechanism,[52] the electrophile approaches the enamine and the new C–C bond formation also results in the ring closure to the bicyclic oxazolidinone. However, the corresponding transition states are around 10 kcal mol^{-1} higher than for the enamine pathway and would not account for the experimentally found stereochemistry.[46] Oxazolidinones are therefore still believed to be in equilibrium with the iminiums but without directly generating enamines.

Thus, to examine the formation of oxazolidinones in the Hajos–Parrish reaction, and the influence of the 4,5 bridges in proline, we calculated the energy profiles and transition states relative to the formation of *endo* and *exo* oxazolidinones from the corresponding *E* and *Z* iminiums, in comparison to L-proline (Fig. 9A, B and Table 5). The *cis*-4,5-ethano-L-proline catalyst **4** stands out of the series, as the *cis*-ethano bridge prevents the formation of the *exo*-oxazolidinones (Fig. 9A),

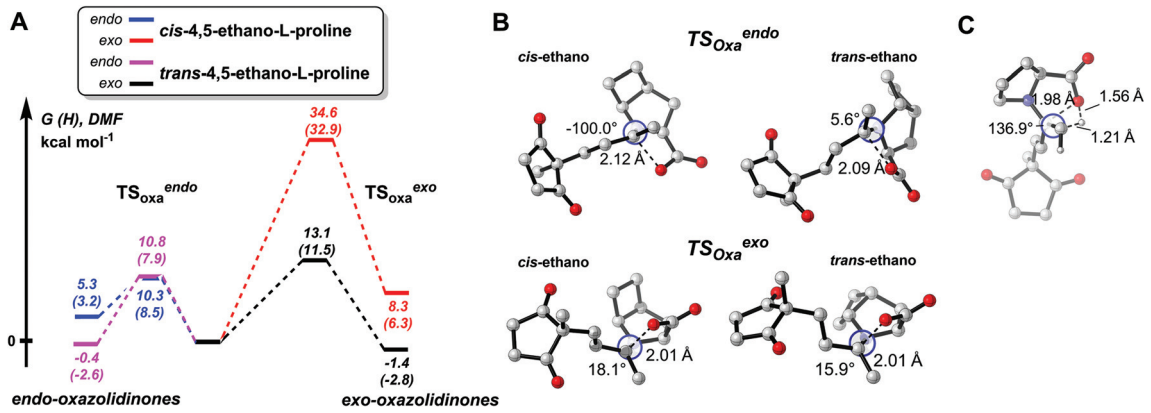

Fig. 9 A. DFT energy profile for the formation of *endo* and *exo* oxazolidinones from the corresponding *E* and *Z* iminiums (ωB97x-D/def2-TZVP). B. Transition states to the *endo* and *exo* oxazolidinones for the *cis*- and *trans*-ethano-proline catalyzed reactions. C. Structure of a presumed transition state for direct conversion of the proline-derived *exo* oxazolidinone to the *anti* enamine.

Table 5 DFT energies for the formation of *endo* and *exo*-oxazolidinones from L-proline and its 4,5-bridged analogues. Iminium energies set to zero

	Iminiums		TS – oxazolidinones		Oxazolidinones	
Entry	*E* (*syn*)	*Z* (*anti*)	*Endo*	*Exo*	*Endo*	*Exo*
L-Proline	0 (0)	0 (0)	11.1 (7.7)	13.1 (10.4)	2.5 (−2.1)	1.6 (−0.8)
cis-Methano	0 (0)	0 (0)	10.4 (7.7)	9.8 (8.0)	0.3 (−2.5)	−2.6 (−4.7)
trans-Methano	0 (0)	0 (0)	11.7 (7.3)	13.6 (11.5)	−0.9 (−4.8)	−2.5 (−5.0)
cis-Ethano	0 (0)	0 (0)	10.3 (8.5)	34.6 (32.9)	5.3 (3.2)	8.3 (6.3)
trans-Ethano	0 (0)	0 (0)	10.8 (7.9)	13.1 (11.5)	−0.4 (−2.6)	−1.4 (−2.8)

because the bridging methylene groups come in close contact to the forming C–O bond (Fig. 9B). The resulting *exo*-oxazolidinone appears unstable (Δ*G* from the corresponding iminium = 8.3 kcal mol^{-1}, see Table 5), while the *endo* isomer produced from the *cis*-ethano-proline is also the less stable cyclized product of the *endo* series (Δ*G* from the corresponding iminium = 5.3 kcal mol^{-1}, see Table 5). The *cis*-ethano bridge could therefore limit the formation of both oxazolidinone species, particularly in the *exo* isomer (Fig. 9A). This is however not reflected in the Hajos–Parrish reaction, as both catalysts produce similar yields and kinetics.

While a probable transition state directly connecting the *exo* oxazolidinone to the enamine has been found (Fig. 9C), it lies high in energy (around 50 kcal mol^{-1} over the oxazolidinone) and thus cannot account for a reasonable pathway (Fig. 9C). Furthermore, two low-lying imaginary frequencies could not be removed. Therefore, as in the 4,5-methano-proline and proline cases, formation of enamines should arise directly from the iminium intermediates when using the 4,5-ethano-prolines as catalysts in the Hajos–Parrish reaction.

Conclusion

We have described the catalytic properties of *cis*- and *trans*-4,5-ethano-L-prolines for the venerable Hajos–Parish intramolecular aldol reaction, together with a detailed analysis of the underlying mechanisms responsible for their catalytic performance. The spatial disposition of the ethano bridge in these new 4,5-bridged proline derivatives relative to the carboxyl group plays a crucial role and contributes to the catalytic and stereocontrolling efficiency of the reaction. Remarkably, the *trans*-4,5-ethano-proline isomer **7** is found to be an excellent catalyst providing 98% ee, in contrast to the poor induction provided by its *cis* isomer (64% ee). In comparison to our previous results with the *cis*- and *trans*-4,5-methano-proline congeners,[22] this is a reversed trend, where the *cis*-methano-proline **4** proved to be a better chiral inducer that the *trans* diastereomer.

These superior chiral induction from the 4,5-*trans*-ethano-proline **7** *versus* the *cis*-isomer were predicted and rationalized by DFT calculations, as evidenced by the activation energies to the *syn*- and *anti*-TS. Further insights into the stabilizing interactions delivering the *anti*-TS selectivity of the reaction are provided by specific calculations of donor–acceptor CT energies and deletions of NBOs. Energy decomposition reveals that the *trans*-4,5-ethano-proline **7** gives enantiomeric purity similar to proline due to a unfavored *syn*-TS in terms of steric repulsions. A high steric repulsion of the *syn*-TS that is only partially balanced by coulombic interactions and orbital interactions, is seen in all the good chiral inducers of the series comprising proline, methano- and ethano-prolines.

Finally, computation of the steps along the reaction pathway involving the formation of the enamines and the "parasitic" oxazolidinones preceding the aldol reaction, shows little influence of the ethano bridge on the overall reactivity in the Hajos–Parrish reaction.

Author contributions

Sofiane Hocine synthesized and characterized the compounds described in this paper and performed the kinetic study. Gilles Berger performed the calculations and analyzed of data. All authors reviewed the manuscript.

Conflicts of interest

There are no conflicts to declare.

Acknowledgements

We thank NSERC for financial assistance. We also thank Thierry Maris and Michel Simard from the X-ray diffraction laboratory of the Université de Montréal for X-ray analysis.

Notes and references

1 Z. G. Hajos and D. R. Parrish, Asymmetric synthesis of bicyclic intermediates of natural product chemistry, *J. Org. Chem.*, 1974, **39**, 1615–1621.
2 Z. G. Hajos and D. R. Parrish, Asymmetric synthesis of optically active polycyclic organic compounds, DE2102623, 1971.
3 U. Eder, G. Sauer and R. Wiechert, New Type of Asymmetric Cyclization to Optically Active Steroid CD Partial Structures, *Angew. Chem., Int. Ed. Engl.*, 1971, **10**, 496–497.
4 S. H. Xiang and B. Tan, Advances in asymmetric organocatalysis over the last 10 years, *Nat. Commun.*, 2020, **11**, 1–5.
5 D. W. C. MacMillan, The advent and development of organocatalysis, *Nature*, 2008, **455**, 304–308.
6 S. Hanessian, S. Giroux and L. B. Merner, *Design and strategy in organic synthesis: from the Chiron approach to catalysis*, Wiley VCH, Weinheim, Germany.R., 2004.
7 R. Mahrwald, *Modern Aldol Reactions*, Wiley-VCH, Weinheim, Germany, 2004.
8 S. Yamada, K. Hiroi and K. Achiwa, Asymmetric synthesis with amino acid I. Asymmetric induction in the alkylation of keto-enamine, *Tetrahedron Lett.*, 1969, **10**, 4233–4236.
9 S. Yamada and G. Otani, Asymmetric Synthesis with Amino Acid. II. Asymmetric Synthesis of Optically Active 4.4-disubstituted-2-cyclohexenone, *Tetrahedron Lett.*, 1969, **10**, 4237–4240.
10 J. F. Schneider, C. L. Ladd and S. Bräse, Proline as an Asymmetric Organocatalyst, in *Sustainable Catalysis: Without Metals or Other Endangered Elements, Part 1*, 2015, ch. 5, pp. 79–119.
11 B. List, R. A. Lerner, C. F. B. Iii, N. Torrey, P. Road, L. Jolla and R. V. December, Proline-Catalyzed Direct Asymmetric Aldol Reactions The Skaggs Institute for Chemical Biology and the Department of Molecular Biology The Scripps Research Institute Most enzymatic transformations have a synthetic counterpart. Often though, the mechanism, *J. Am. Chem. Soc.*, 2000, **122**, 2395–2396.
12 S. Mukherjee, J. W. Yang, S. Hoffmann and B. List, Asymmetric enamine catalysis, *Chem. Rev.*, 2007, **107**, 5471–5569.
13 B. List, The ying and yang of asymmetric aminocatalysis, *Chem. Commun.*, 2006, 819–824.
14 S. Bahmanyar and K. N. Houk, The origin of stereoselectivity in proline-catalyzed intramolecular aldol reactions, *J. Am. Chem. Soc.*, 2001, **123**, 12911–12912.
15 B. List, L. Hoang and H. J. Martin, New mechanistic studies on the proline-catalyzed aldol reaction, *Proc. Natl. Acad. Sci. U. S. A.*, 2004, **101**, 5839–5842.
16 S. Bahmanyar, K. N. Houk, H. J. Martin and B. List, Quantum mechanical predictions of the stereoselectivities of proline-catalyzed asymmetric intermolecular aldol reactions, *J. Am. Chem. Soc.*, 2003, **125**, 2475–2479.
17 A. Armstrong, R. A. Boto, P. Dingwall, J. Contreras-García, M. J. Harvey, N. J. Mason and H. S. Rzepa, The Houk-List transition states for organocatalytic mechanisms revisited, *Chem. Sci.*, 2014, **5**, 2057–2071.
18 K. N. Rankin, J. W. Gauld and R. J. Boyd, Density functional study of the proline-catalyzed direct aldol reaction, *J. Phys. Chem. A*, 2002, **106**, 5155–5159.
19 U. I. Tafida, A. Uzairu and S. E. Abechi, Mechanism and rate constant of proline-catalysed asymmetric aldol reaction of acetone and p-nitrobenzaldehyde in solution medium: Density-functional theory computation, *J. Adv. Res.*, 2018, **12**, 11–19.
20 F. R. Clemente and K. N. Houk, Computational evidence for the enamine mechanism of intramolecular aldol reactions catalyzed by proline, *Angew. Chem., Int. Ed.*, 2004, **43**, 5766–5768.
21 F. R. Clemente and K. N. Houk, Theoretical studies of stereoselectivities of intramolecular aldol cyclizations catalyzed by amino acids, *J. Am. Chem. Soc.*, 2005, **127**, 11294–11302.
22 P. H. Y. Cheong, K. N. Houk, J. S. Warrier and S. Hanessian, Catalysis of the Hajos-Parrish-Eder-Sauer-Wiechert reaction by cis- and trans-4,5-methanoprolines: Sensitivity of proline catalysis to pyrrolidine ring conformation, *Adv. Synth. Catal.*, 2004, **346**, 1111–1115.
23 P. H. Y. Cheong and K. N. Houk, Origins and predictions of stereoselectivity in intramolecular aldol reactions catalyzed by proline derivatives, *Synthesis*, 2005, 1533–1537.
24 S. Hanessian, U. Reinhold and G. Gentile, The Synthesis of Enantiopure Acids by a Novel Cyclopropanation Reaction: The "Flattening" of Proline, *Angew. Chem., Int. Ed. Engl.*, 1997, **36**, 1881–1884.

25 S. Hanessian, U. Reinhold and S. Claridge, Probing the importance of spacial and conformational domains in captopril analogs for angiotensin converting enzyme activity, *Bioorg. Med. Chem. Lett.*, 1998, **8**, 2123–2128.
26 J. Yu, V. Truc, P. Riebel, E. Hierl and B. Mudryk, One-Pot Conversion of Lactam Carbamates To Cyclic Enecarbamates: Preparation of 1-Tert-Butoxycarbonyl-2,3-Dihydropyrrole, *Org. Synth.*, 2008, **85**, 64–71.
27 G. Wang, C. A. James, N. A. Meanwell, L. G. Hamann and M. Belema, A scalable synthesis of (1R,3S,5R)-2-(tert-butoxycarbonyl)-2-azabicyclo[3.1.0]hexane-3-carboxylic acid, *Tetrahedron Lett.*, 2013, **54**, 6722–6724.
28 G. Berger, M. Vilchis-Reyes and S. Hanessian, Structural Properties and Stereochemically Distinct Folding Preferences of 4,5-cis and trans-Methano-L-Proline Oligomers: The Shortest Crystalline PPII-Type Helical Proline-Derived Tetramer, *Angew. Chem., Int. Ed.*, 2015, **54**, 13268–13272.
29 M. A. Vilchis-Reyes and S. Hanessian, in *Proline Methanologues: Design, Synthesis, Structural Properties, and Applications in Medicinal Chemistry*, Topics in Heterocyclic Chemistry, Springer Berlin Heidelberg, 2016, pp. 1–45.
30 G. Berger, I. Chab-Majdalani and S. Hanessian, Properties of the amide bond involving proline 4,5-methanologues: an experimental and theoretical study, *Isr. J. Chem.*, 2017, **57**, 292–302.
31 M. Baranac-Stojanović and M. Stojanović, ^{1}H NMR chemical shifts of cyclopropane and cyclobutane: A theoretical study, *J. Org. Chem.*, 2013, **78**, 1504–1507.
32 R. Balasubramanian, A. V. Lakshminarayanan, M. N. Sabesan, G. Tegoni, K. Venkatesan and G. N. Ramachandran, Studies on the conformation of amino acids. VI. Conformation of the proline ring as observed in crystal structures of amino acids and peptides, *Int. J. Protein Res.*, 1971, **3**, 25–33.
33 G. N. Ramachandran, A. V. Lakshminarayanan, R. Balasubramanian and G. Tegoni, Studies on the conformation of amino acids XII. Energy calculations on prolyl residue, *Biochim. Biophys. Acta, Protein Struct.*, 1970, **221**, 165–181.
34 D. Iwan, K. Kamińska and E. Wojaczyńska, Application of polyamines and amino acid derivatives based on 2-azabicycloalkane backbone in enantioselective aldol reaction, *Molecules*, 2021, **26**, 5166.
35 C. B. Shinisha and R. B. Sunoj, Bicyclic proline analogues as organocatalysts for stereoselective aldol reactions: an in silico DFT study, *Org. Biomol. Chem.*, 2007, **5**, 1287–1294.
36 J.-D. Chai and M. Head-Gordon, Long-range corrected hybrid density functionals with damped atom-atom dispersion corrections, *Phys. Chem. Chem. Phys.*, 2008, **10**, 6615–6620.
37 F. Weigend and R. Ahlrichs, Balanced basis sets of split valence, triple zeta valence and quadruple zeta valence quality for H to Rn: Design and assessment of accuracy, *Phys. Chem. Chem. Phys.*, 2005, **7**, 3297–3305.
38 F. Weigend, Accurate Coulomb-fitting basis sets for H to Rn, *Phys. Chem. Chem. Phys.*, 2006, **8**, 1057–1065.
39 E. D. Glendening, J. K. Badenhoop, A. E. Reed, J. E. Carpenter, J. A. Bohmann, C. M. Morales, C. R. Landis and F. Weinhold, *NBO 6.0*, Theor. Chem. Institute, Univ. Wisconsin, Madison, WI.
40 F. Neese, A. Hansen and D. G. Liakos, Efficient and accurate approximations to the local coupled cluster singles doubles method using a truncated pair natural orbital basis, *J. Chem. Phys.*, 2009, **131**, 064103.
41 F. Neese, A. Hansen, F. Wennmohs and S. Grimme, Accurate theoretical chemistry with coupled pair models, *Acc. Chem. Res.*, 2009, **42**, 641–648.
42 C. Riplinger and F. Neese, An efficient and near linear scaling pair natural orbital based local coupled cluster method, *J. Chem. Phys.*, 2013, **138**, 034106.
43 J. K. Badenhoop and F. Weinhold, Natural bond orbital analysis of steric interactions, *J. Chem. Phys.*, 1997, **107**, 5406–5421.
44 J. K. Badenhoop and F. Weinhold, Natural steric analysis of internal rotation barriers, *Int. J. Quantum Chem.*, 1999, **72**, 269–280.
45 F. Weinhold and C. R. Landis, *Discovering Chemistry With Natural Bond Orbitals*, Wiley, 2012.
46 A. K. Sharma and R. B. Sunoj, Enamine versus oxazolidinone: What controls stereoselectivity in proline-catalyzed asymmetric aldol reactions?, *Angew. Chem., Int. Ed.*, 2010, **49**, 6373–6377.
47 T. Kanzian, S. Lakhdar and H. Mayr, Kinetic evidence for the formation of oxazolidinones in the stereogenic step of proline-catalyzed reactions, *Angew. Chem., Int. Ed.*, 2010, **49**, 9526–9529.
48 P. Renzi, J. Hioe and R. M. Gschwind, Enamine/Dienamine and Brønsted Acid Catalysis: Elusive Intermediates, Reaction Mechanisms, and Stereoinduction Modes Based on in Situ NMR Spectroscopy and Computational Studies, *Acc. Chem. Res.*, 2017, **50**, 2936–2948.
49 D. Seebach, A. K. Beck, D. M. Badine, M. Limbach, A. Eschenmoser, A. M. Treasurywala, R. Hobi, W. Prikoszovich and B. Linder, Are oxazolidinones really unproductive, parasitic species in proline catalysis? - Thoughts and experiments pointing to an alternative view, *Helv. Chim. Acta*, 2007, **90**, 425–471.
50 H. Iwamura, D. H. Wells, S. P. Mathew, M. Klussmann, A. Armstrong and D. G. Blackmond, Probing the active catalyst in product-accelerated proline-mediated reactions, *J. Am. Chem. Soc.*, 2004, **126**, 16312–16313.
51 M. H. Haindl, J. Hioe and R. M. Gschwind, The Proline Enamine Formation Pathway Revisited in Dimethyl Sulfoxide: Rate Constants Determined via NMR, *J. Am. Chem. Soc.*, 2015, **137**, 12835–12842.
52 D. Seebach, M. Boes, R. Naef and W. B. Schweizer, Alkylation of Amino Acids without Loss of the Optical Activity: Preparation of -Substituted Proline Derivatives. A Case of Self-Reproduction of Chirality, *J. Am. Chem. Soc.*, 1983, **105**, 5390–5398.